Proceedings of the 2004 IEEE
International Conference on Control Applications
Taipei, Taiwan, September 2-4, 2004

Integrated longitudinal and lateral control for vehicle low speed automation

Saïd Mammar and Mariana Netto

***Abstract*— This paper proposes and evaluates an integrated longitudinal and lateral control for vehicles low speed automation. The automation is dedicated to sub-urban congested highways. Using a simplified coupled longitudinal/lateral model, we provide a solution for the vehicle following problem using first and second order sliding mode controls. The performances of the synthesized control laws are highlighted by several simulation tests.**

***Index Terms*— Lateral dynamics, Vehicle following, Sliding mode control, Chattering, Twisting Algorithm.**

I. Introduction

The intense urbanization of these 40 last years led to a broad peripheral extension of the old European metropolises but also to the development of increasingly distant zones of activities and live. This generated simultaneously the increase of interurban displacements and the covered distances. The current averages are at the neighborhoods of 40 km and 1 hour by way. In spite of the actions taken to limit the displacements, in particular inside the cities, the car remains the best adapted means of transport. The disparate perish-urban zones are indeed not very favorable for heavy collective transport. Another idea for better managing the recurring congestions would be to allow an automation at low speed of the vehicles. It should be noted that in normal steady state driving conditions, the traffic capacity of a lane is around 2200 vehicles per hour on peri-urban motorways. However during congested situations, this value does not last and capacity generally falls with only 1200 vehicle per hour [1], [7], [3]. This traffic jam generates also drivers' displeasure and irritation. Then, as far as car drivers are concerned, it is advisable to find solutions to such a growing problem. The goal here is to better manage the behavior of ground vehicles in order to increase traffic capacity while improving safety and comfort aspects ensuring then a guaranteed travel time. In this paper, combined longitudinal and lateral control strategies are considered using sliding mode control techniques. A constant headway time policy is adopted for the longitudinal control while leader trajectory following is adopted for the lateral part. While the proposed method also works for high speed, we voluntarily limit the speed. The remainder of the paper is organized as follows: section 2 gives the vehicle dynamic model and the positioning equation relative to the leader. A first order sliding mode control is synthesized and evaluated in section 3. This control approach is then enhanced using second order sliding mode in section 4 [5], [2]. Simulation results obtained in different situations highlight the robustness of the second order approach.

S. Mammar is with Université d'Évry val d'Essonne, France. LSC-CNRS-FRE 2494, 40 rue du Pelvoux CE1455, 91025, Evry, Cedex mammar@iup.univ-evry.fr

M. Netto, is with INRETS/LCPC - LIVIC Laboratoire sur les Interactions Véhicule-Infrastructure-Conducteur, 14, route de la Minière, Bât 824, 78000, Versailles, France. netto@lcpc.fr

II. Vehicle modelling

The vehicle model is restricted to the longitudinal, lateral and yaw rotational motions. The longitudinal motion is controlled by means of the composite torque T_c on the wheels. This torque is an engine torque when it is positive or a brake torque otherwise. The control of the yaw and lateral translation motions is done by the front wheels steering angle δ_f.

Table 1: Vehicle parameters

T_c	equivalent drive and brake torque
T_{rr}	rolling resistance torque
δ_f	front wheels steering angle
c_f/c_r	front and rear cornering stiffness
F_{yf}/F_{yr}	front and rear tire lateral forces
l_f/l_r	distance to CG of front and rear axle
α_f/α_r	front/rear tire slip angle
I_z	Yaw inertia
I_{eff}	wheel effective inertia
m	vehicle mass
C_x/C_y	longitudinal and lateral air drag coefficient

In the following, the indices (l,s,r) denote leader vehicle, follower vehicle and relative data, respectively. The road is assumed to be plane without gradient or superelevation. The vehicle simplified model is given by the following three equations [4]

$$\begin{cases} \dot{v}_{x_s} = \frac{T_c - T_{rr}}{I_{eff}} - \frac{C_x v_{x_s}^2}{m} + v_{y_s}\dot{\psi}_s \\ \dot{v}_{y_s} = \frac{F_{y_f} + F_{y_r} - C_y v_{y_s}^2}{m} - v_{x_s}\dot{\psi}_s \\ \ddot{\psi}_s = \frac{1}{I_z}\left[l_f F_{y_f} - l_r F_{y_r}\right] \end{cases}$$

The first equation represents the dynamics of the longitudinal translation motion. The second one gives the lateral translation dynamics while the last one provides the yaw motion. The terms $v_{y_s}\dot{\psi}_s$ and $v_{x_s}\dot{\psi}_s$ represent the coupling between the two translational motions. In this simplified model, it is assumed that the longitudinal motion has no

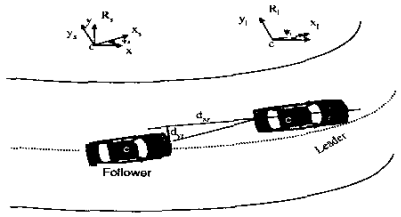

Fig. 1. Follower vehicle positioning relative to the leader

slipping. The lateral motion,however, is governed by tires lateral forces which are proportional to the front and rear tires slip angles α_f and α_r: $F_{y_f} = 2c_f\alpha_f$ and $F_{yr} = 2c_r\alpha_r$. The slip angles are computed from the angle of the speed vector at the tire-pavement contact. Under small angles assumption, one can get

$$\alpha_f = \delta_f - \frac{v_{y_s} + l_f\dot{\psi}_s}{v_{x_s}}, \quad \alpha_r = -\frac{v_{y_s} - l_r\dot{\psi}_s}{v_{x_s}}$$

The model is finally put under the canonical form

$$\begin{cases} \dot{v}_{x_s} = f_0 + g_0 T_c \\ \dot{v}_{y_s} = f_1 + g_1\delta_f \\ \ddot{\psi}_s = f_2 + g_2\delta_f \end{cases} \tag{1}$$

with

$$\begin{cases} f_0 = -\frac{T_{tr}}{I_{eff}} - \frac{C_x v_{x_s}^2}{m} + v_{y_s}\dot{\psi}_s \\ g_0 = \frac{1}{I_{eff}} \\ f_1 = \frac{-2c_f}{m}\frac{v_{y_s} + l_f\dot{\psi}_s}{v_{x_s}} - \frac{2c_r}{m}\frac{v_{y_s} - l_r\dot{\psi}_s}{v_{x_s}} - \frac{C_y v_{y_s}^2}{m} - v_{x_s}\dot{\psi}_s \\ f_2 = \frac{-l_f}{I_z}2c_f\frac{v_{y_s} + l_f\dot{\psi}_s}{v_{x_s}} + \frac{l_r}{I_z}2c_r\left(\frac{v_{y_s} - l_r\dot{\psi}_s}{v_{x_s}}\right) \\ g_0 = \frac{1}{I_{eff}}, \quad g_1 = 2c_f, \quad g_2 = \frac{l_r}{I_z}2c_f \end{cases} \tag{2}$$

Notice that these equations are written in the follower vehicle body coordinates. Similar equations can be developed for the leader vehicle or any other one in case of a string of several vehicles.

III. Absolute and Relative Vehicle Positioning

The follower vehicle is initially at the origin of the absolute frame with an initial yaw angle $\psi_s(0)$. Its current absolute position and the yaw angle are then

$$\begin{cases} \psi_s = \int_0^t \dot{\psi}_s d\tau + \psi_s(0) \\ x_s(t) = \int_0^t (v_{x_s}\cos\psi_s - v_{y_s}\sin\psi_s)\, d\tau \\ y_s(t) = \int_0^t (v_{x_s}\sin\psi_s + v_{y_s}\cos\psi_s)\, d\tau \end{cases}$$

Using the same procedure with the preceding vehicle, one can get the triplet (x_l, y_l, ψ_l). The goal now is to express the lateral deviation of the follower vehicle d_{yr} and its spacing with respect to the preceding one d_{xr} as shown in figure 1. They are obtained by writing the relative position of the follower vehicle

$$\begin{bmatrix} d_{xr} \\ d_{yr} \end{bmatrix} = R(\psi_l)\left(\begin{bmatrix} x_s + l_f\cos\psi_s \\ y_s + l_f\sin\psi_s \end{bmatrix} - \begin{bmatrix} x_l - l_r\cos\psi_l \\ y_l - l_r\sin\psi_l \end{bmatrix}\right)$$

where $R(\psi_l)$ is the rotation matrix concerning the angle ψ_l. By derivation, the previous equations give us $\dot{d}_{xr}$ and $\dot{d}_{yr}$

$$\begin{cases} \dot{d}_{xr} = -v_{x_l} + d_{yr}\dot{\psi}_l + v_{x_s}\cos\psi_r + (v_{y_s} + \dot{\psi}_s l_f)\sin\psi_r \\ \dot{d}_{yr} = -v_{y_l} + (l_r - d_{xr})\,\dot{\psi}_l - v_{x_s}\sin\psi_r + \\ (v_{y_s} + \dot{\psi}_s l_f)\cos\psi_r \end{cases}$$

At this stage, it is necessary to perform a second derivation so that the two control inputs T_c and δ_f appear in the equations. By proceeding like this, we obtain

$$\begin{cases} \ddot{d}_{xr} = a_0 + b_0 T_c + c_0\delta_f \\ \ddot{d}_{yr} = a_1 + b_1 T_c + c_1\delta_f \end{cases}$$

with

$$\begin{cases} a_0 = -\dot{v}_{x_l} + d_{yr}\ddot{\psi}_l + \dot{d}_{yr}\dot{\psi}_l + f_0\cos\psi_r - v_{x_s}\sin\psi_r\dot{\psi}_r \\ + (v_{y_s} + \dot{\psi}_s l_f)\cos\psi_r\dot{\psi}_r + (f_1 + f_2 l_f)\sin\psi_r \\ b_0 = g_0\cos\psi_r \\ c_0 = (g_1 + g_2 l_f)\sin\psi_r \\ a_1 = -\dot{d}_{xr}\dot{\psi}_l - d_{xr}\ddot{\psi}_l - (\dot{v}_{y_l} - \ddot{\psi}_l l_r) - f_0\sin\psi_r - \\ (v_{ys} + l_f\dot{\psi}_s)\,\dot{\psi}_r\sin\psi_r + (f_1 + f_2 l_f - v_{x_s}\dot{\psi}_r)\cos\psi_r \\ b_1 = -g_0\sin\psi_r \\ c_1 = (g_1 + g_2 l_f)\cos\psi_r \end{cases}$$

IV. First Order Sliding Mode Control

A. Design methodology

We develop in this section first and second order sliding mode control laws for both longitudinal and lateral control. The procedure assumes that the vehicles are equipped with all necessary sensors and communication means. We proceed as follows

- for the longitudinal control we adopt a constant headway time policy. The sliding surface is chosen as

  $$S_{long} = \sigma_{long}$$

  with $\sigma_{long} = d_{x_r} + (d_0 + hv_{x_s})$ where d_0 represents the inter-distance while stopping and h is the headway time. This surface S_{long} was chosen because of the recent French law that specifies that drivers are not allowed to drive with a headway time less than 2 seconds.
- For the lateral control, a vehicle following policy is chosen. The control goal is thus to minimize a mixed criteria between follower vehicle lateral displacement and relative yaw angle. This criteria is $\sigma_{lat} = d_{y_r} + \lambda\psi_r$. The weighting factor λ allows to favor one component against the other. The sliding surface is finally

  $$S_{lat} = \dot{\sigma}_{lat} + s_1\sigma_{lat} + s_2\int_0^t \sigma_{lat} d\tau \tag{3}$$

The sliding surface is $S = [S_{long}, S_{lat}]^T$. The equivalent control input is first computed from $\dot{S} = [\dot{S}_{long}, \dot{S}_{lat}]^T = 0$, as follows

$$\dot{S} = \begin{bmatrix} \dot{d}_{xr} + h\dot{v}_{x_s} \\ \left(\ddot{d}_{y_r} + \lambda\ddot{\psi}_r\right) + s_1\left(\dot{d}_{y_r} + \lambda\dot{\psi}_r\right) + s_2\left(d_{y_r} + \lambda\psi_r\right) \end{bmatrix} \quad (4)$$

$$= G + B\begin{bmatrix} T_c \\ \delta_f \end{bmatrix} \quad (5)$$

where

$$G = \begin{bmatrix} \dot{d}_{xr} + hf_0 \\ a_1 + \lambda(\ddot{\psi}_l - f_2) + s_1\left(\dot{d}_{y_r} + \lambda\dot{\psi}_r\right) + s_2\left(d_{y_r} + \lambda\psi_r\right) \end{bmatrix}$$

$$B = \begin{bmatrix} hg_0 & 0 \\ b_1 & c_1 - \lambda g_2 \end{bmatrix}$$

The equivalent longitudinal and lateral control inputs are thus

$$\begin{bmatrix} T_{ceq} \\ \delta_{feq} \end{bmatrix} = -B^{-1}G$$

By choosing a constant and proportional sliding approach, one finally obtain

$$\begin{bmatrix} T_c \\ \delta_f \end{bmatrix} = \begin{bmatrix} T_{ceq} \\ \delta_{feq} \end{bmatrix} - k_1 sign(S) - k_2 S \quad (6)$$

Comparatively to the constant reaching law, this reaching law introduces a supplementary degree of freedom. In fact, when the system is far from the sliding manifold, the behavior is dominated by the k_2 term, where the k_1 term becomes dominant when approaching the manifold. A good choice of k_1 and k_2 will thus allows to reduce both the convergence time and the well-known chattering phenomena near the sliding manifold.

B. Simulation tests

It is important to remind that the vehicle following problem considered here is dedicated to low speed automation in congested sub-urban highways. The developed longitudinal and lateral control laws have to cover all operational speeds including stop-and-go traffic conditions. The speed is however limited to 60km/h for safety reasons. The maneuvers of the leader include acceleration, braking and lane change.

1) Follower cut in maneuver: We consider first that the two vehicles are at the same speed of 60km/h on a two lanes straight road section. The leader is on the center of the right lane while the follower is on the center of the left one. The lateral spacing is thus of 3m, which corresponds to the assumed lane width. In addition, the longitudinal spacing is 27.5m. At time $t = 0$sec, the follower initiates a cut in manoeuver to the right lane. However, it has also to perform braking as the actual spacing is smaller by 10.82m than the desired spacing of 38.32m which corresponds to a headway time of 2sec. The longitudinal and lateral positions of the vehicles appear in figure 2. It can be easily seen that the cut in maneuver is performed without overshot. The lateral steady state error is about 1.5cm. Figure 3 shows the phase portrait $\left(S_{lat}, \dot{S}_{lat}\right)$ which proves the convergence to the sliding manifold. One can also note that the vehicle occupants comfort is preserved, as attested by the limited values of the lateral speed and acceleration given in figures 4 and 5. However, the existence of the high frequency chattering phenomenon on both the lateral acceleration and the steering angle (figure 5 and 6) may lead to comfort degradation. The longitudinal speed is shown in figure 7. While the leader is cruising, the follower performs a braking maneuver during a first phase and an acceleration in a second phase. There is no overshot in the speed and the relative speed is zero at steady state. The absence of overshot is very important from the safety point of view, it ensures that the time to collision is always infinite. Finally, figure 8 shows the evolution in time of the sliding manifold which we will denote, from now on, the spacing error. It

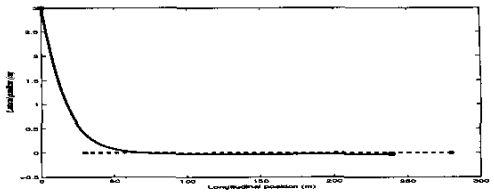

Fig. 2. Cut in maneuver of the follower lateral and longitudinal positions of the leader (-.) and the follower (-).

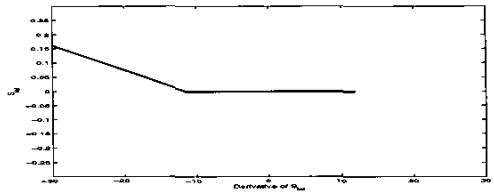

Fig. 3. Cut in maneuver: Phase portrait of the lateral sliding surface S_{lat}

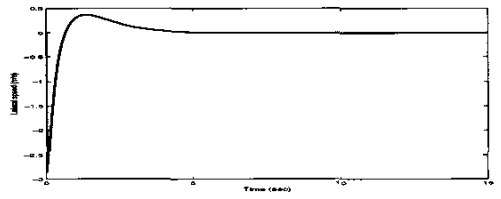

Fig. 4. Cut in maneuver: follower vehicle lateral speed

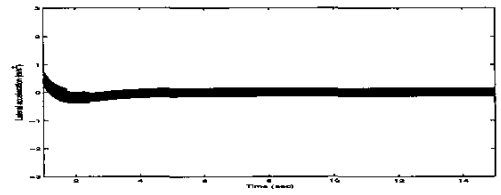

Fig. 5. Cut in maneuver: follower vehicle lateral acceleration

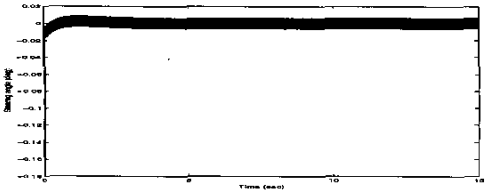

Fig. 6. Cut in maneuver: follower vehicle steering angle

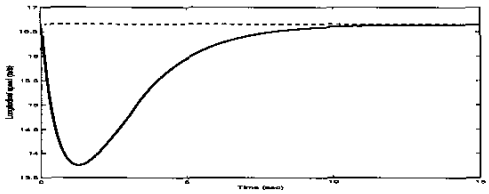

Fig. 7. Cut in maneuver: Leader (-.) and follower (-) longitudinal speed

can be seen that the desired spacing distance is reached. The corresponding composite (engine/brake) torque is shown in figure 9. It can be noted noted that it exhibits chattering when approaching the steady state value that compensates the rolling resistance torque.

2) Heading variation: The vehicles are initially aligned on the same lane. The initial spacing is still of 20m. 40 meters later, the leader performs a heading change of $\psi_l = 0.1$rad. We remark in figure 10 that the follower reacts efficiently to this maneuver. The lateral spacing converges to zero very fast. Figure 11 shows the results obtained when the two previous maneuvers are combined. The controller is still performing.

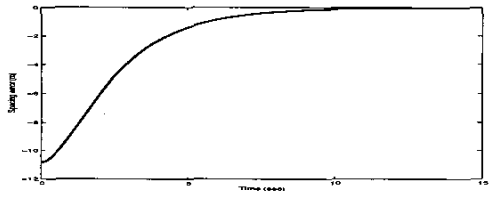

Fig. 8. Cut in maneuver: Spacing error

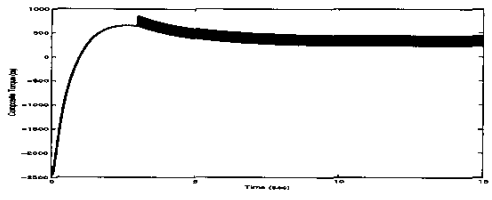

Fig. 9. Cut in maneuver: Composite (engine / brake) torque

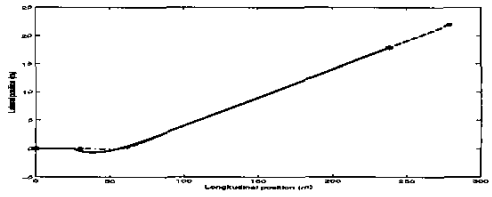

Fig. 10. Leader vehicle heading change: Positions of leader (-.) and the follower (-)

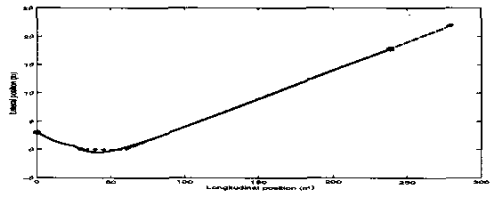

Fig. 11. Cut in maneuver combined with leader vehicle heading change: Positions of leader (-.) and the follower (-)

V. Enhancement by second order sliding mode control

The first order sliding mode control procedure already presents good properties. Enhancement is explored here by means of a second order sliding mode, especially using Twisting Algorithm.

A. Methodology

The Twisting Algorithm is applied to the input derivatives $\dot{T}_c$ and $\dot{\delta}_f$. The integral actions will smooth the evolution of the plant real control input. The algorithm is as follows

$$\dot{u} = \begin{cases} -u & if \quad |u| > |u_{eq}| \\ -K_M sign(S_i) & if \quad S_i\dot{S}_i > 0, \quad |u| \leq |u_{eq}| \\ -k_m sign(S_i) & if \quad S_i\dot{S}_i \leq 0, \quad |u| \leq |u_{eq}| \end{cases} \tag{7}$$

where $(\dot{u}, u, \dot{S}_i, S_i, u_{eq})$ is either $(\dot{T}_c, T_c, \dot{S}_{long}, S_{long}, T_{c_{eq}})$ or $(\dot{\delta}_f, \delta_f, \dot{S}_{lat}, S_{lat}, \delta_{f_{eq}})$, and k_m and K_M are constants which verify the following inequalities

$$K_M > k_m > 0, k_m > \frac{4C_M}{c_0} \qquad k_m > \frac{C_0}{c_m}, K_M > \frac{C_M}{c_m} + \frac{2C_0}{c_m} \tag{8}$$

where C_M, C_0, c_m and c_0 are deduced from conditions that make possible the application of the algorithm [8].

B. Simulation results

Results obtained for the same maneuvers as for the first order sliding mode appear on figures 12 to 19. Due to space limitation, some figures are omitted. The following remarks can be deduced

- Maneuvers are practically performed in the same manner considering transient phases and tracking errors,

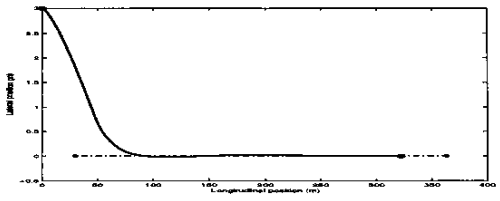

Fig. 12. Cut in maneuver using second order sliding mode; longitudinal and lateral positions of the leader (-.,*) and the follower (-, o).

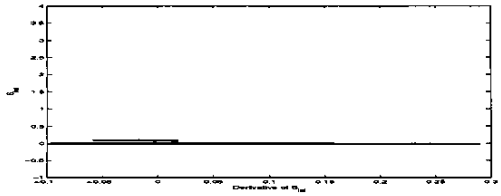

Fig. 13. Cut in maneuver using second order silding mode: $(\dot{S}_{lat}, S_{lat})$

- the lateral acceleration has been smoothed. Better comfort is thus expected,
- control signals do not present chattering phenomena.

These simulation results highlight that the use of second order sliding mode controller enhances considerably the performance of the system.

VI. Robustness analysis

The robustness of the second order sliding mode controller is tested in several configurations such as road adhesion variation and speed variation. The chosen road section is constituted by a 30m of straight line followed by and a circular arc of 200m radius. It ends by a straight section. The trajectories of both vehicles in nominal conditions appear in figure 20.

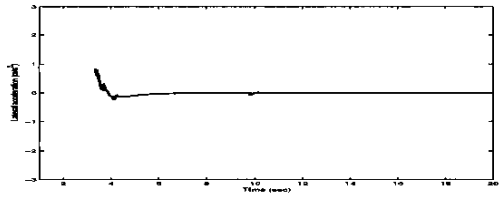

Fig. 14. Cut in maneuver using second order silding mode: Follower lateral acceleration

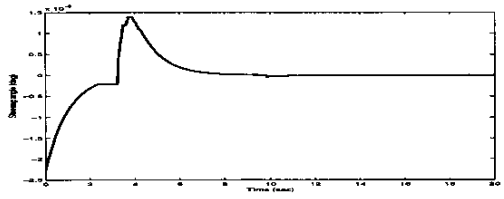

Fig. 15. Cut in maneuver using second order silding mode: Follower steering angle

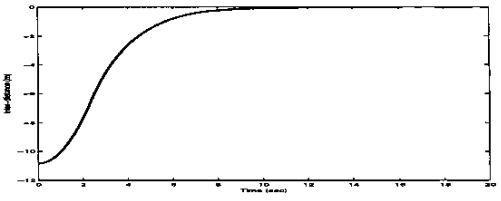

Fig. 16. Cut in maneuver using second order sliding mode: Longitudinal spacing error

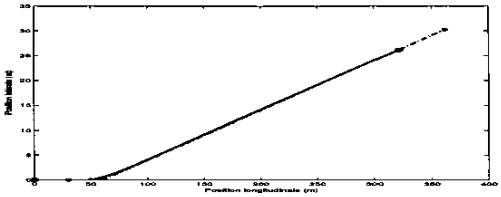

Fig. 17. Second order sliding mode, leader vehicle heading change: Positions of leader (-.) and follower vehicle (-).

A. Road adhesion variation

For this test, the tire stiffness coefficients c_f and c_r are reduced to 70% of their nominal values. This corresponds to a road adhesion of 0.7 instead of 1. The control law is still computed under the assumption of full road adhesion as no measurement of this quantity is available, but the follower vehicle model is simulated with the real adhesion. The results shown in figure 21 still show good vehicle

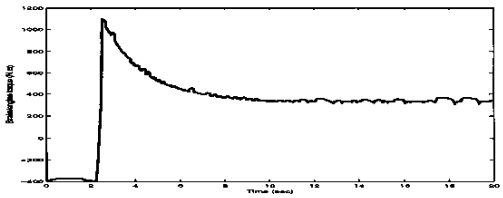

Fig. 18. Brake and engine torque

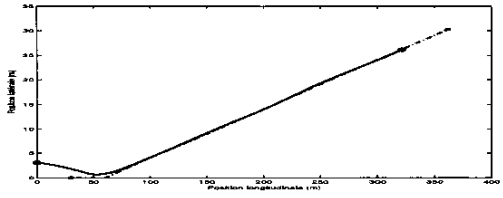

Fig. 19. Second order sliding mode, lane change maneuver and leader vehicle heading change: Positions of leader (-.) and follower vehicle (-).

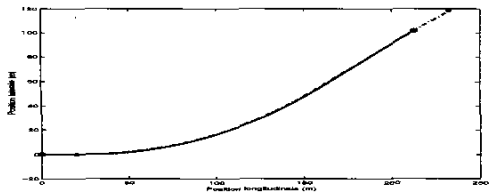

Fig. 20. Trajectories of both vehicle in nominal conditions using second order sliding mode

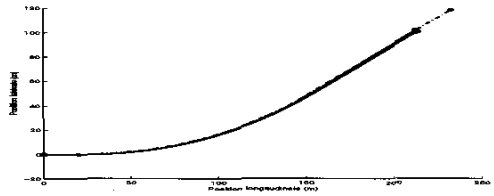

Fig. 21. Road adhesion effect

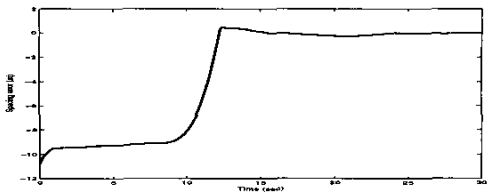

Fig. 23. Second order sliding mode controller, speed variation: Spacing error

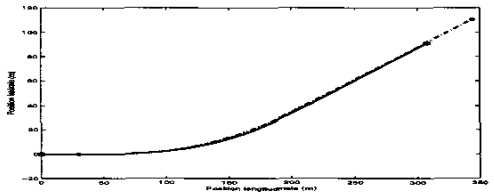

Fig. 24. Second order sliding mode, speed variation: Leader (-.) and follower (-) longitudinal and lateral positions

tracking, however, as the road adhesion is reduced, the performance is gradually deteriorated. It is thus necessary to have an estimate of the road adhesion in order to cover all weather conditions. A simulation study revealed that a rough estimation of about 20% of accuracy is sufficient.

B. Leader speed variation

In this case, the leading vehicle brakes until a longitudinal speed of 2km/h is reached, it then accelerates until the cruising speed of 60km/h is reached again. The speed profile is shown in figure 22. In the same figure the follower longitudinal speed plot shows that the longitudinal controller performs well, the shape is comparable to that of the leader and the steady state error is zero. In addition, the spacing error and the vehicles path presented in figures 23 and 24 show that the longitudinal and lateral controls are not sensitive to speed variations since the maneuver was performed just as well as in the nominal case.

VII. Conclusion

In this paper, a combined longitudinal and lateral control strategy has been developed for low speed road vehicles automation. First and second order sliding mode control methods are used. While both methods show good tracking results, the use of second order sliding mode enhances driving comfort by chattering elimination. This method presents also good robustness properties.

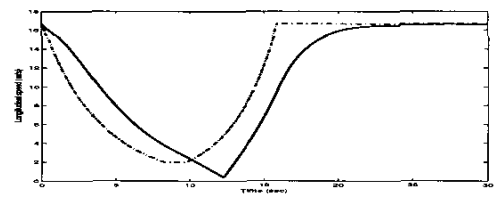

Fig. 22. Second order sliding mode, speed variation: Leader (-.) and follower (-) longitudinal speed

References

[1] S. Mammar et al., *Route automatisée : Analyse et Evaluation d'un Scénario d'Autoroute Péri-urbaine*, Convention DSCR N°9770013, Nov 1999.

[2] S.V. Emelyanov, S.K. Korovin, L.V. Levantovsky, *Second order sliding modes in controlling uncertain systems*, Soviet Jour. of Computer and System Science, 24(4):63-68, 1986.

[3] J. Sainte-Marie, S. Mammar, L. Nouvelière, V. Rouault, "Sub-optimal longitudinal control of road vehicles", ASME, Journal of System Dynamics and Control, à paraître, 2003.

[4] S. Mammar, et Koenig, D., "Vehicle Handling improvement by Active Steering", Vehicle System Dynamics, vol 38, No3, 211-242, 2002.

[5] L.V. Levantovsky, *Second order sliding algorithms : their realization in dynamic of heterogeneous systems*, Institute for System Studies, Moscow, pages 32-43, 1985.

[6] A. Levant, *Sliding order and sliding accuracy in sliding mode control*, Int. Jour. of Cont., 58(6):1247-1263, 1993.

[7] L. Nouvelière, J. Sainte-Marie, S. Mammar, *Modelling, estimation and analysis of inter-vehicular spacing during congested situations*, submitted to IEEE Transaction on Intelligent Transportation Systems.

[8] L. Nouvelière, Mammar, S., et Sainte-Marie, J., "Longitudinal Control of Low Speed Automated Vehicles Using a Second Order Sliding Mode Control ", IEEE-IV'2001, Intelligent Vehicles Symposium, 2001.

[9] R. Labayrade, D. Aubert, J.P. Tarel, Realtime obstacle detection on non flat road geometry through " V-disparity " representation, IEEE Intelligent Vehicle Symposium IV2002, Versailles, France, June 2002.

Numerical values

$T_{rr} = 300N.m$, $c_f = 57.5KN/rad$, $c_r = 57.5KN/rad$, $C_x = 0.35N.s^2m^{-2}$, $C_y = 0.45N.s^2m^{-2}$ $l_f = 1m$, $l_r = 1.5m$, $m = 1500kg$, $I_z = 2500kg.m^2$, $I_{eff} = 0.3 \times m$, $s_1 = 1$, $s_2 = 0.01$ $\lambda = 0.1$, $k_1 = diag\{10^2, 10^{-4}\}$, $k_2 = diag\{250, 10^{-3}\}$, $K_M = \{10^4, 8 \times 10^{-4}\}$, $k_m = \{20, 2 \times 10^{-6}\}$